9928 *Inorg. Chem.* **2010**, *49*, 9928–9939
DOI: 10.1021/ic101133w

Inorganic Chemistry
Article

Eu(III) Complexes of Functionalized Octadentate 1-Hydroxypyridin-2-ones: Stability, Bioconjugation, and Luminescence Resonance Energy Transfer Studies

Evan G. Moore, Jide Xu, Christoph J. Jocher, Todd M. Corneillie, and Kenneth N. Raymond*

Department of Chemistry, University of California, Berkeley, California 94720-1460, and Chemical Science Division, Glenn T. Seaborg Center, Lawrence Berkeley National Laboratory, Berkeley, California 94720

Received June 4, 2010

The synthesis, stability, and photophysical properties of several Eu(III) complexes featuring the 1-hydroxypyridin-2-one (1,2-HOPO) chelate group in tetradentate and octadentate ligands are reported. These complexes pair highly efficient emission with exceptional stabilities (pEu $\sim$ 20.7−21.8) in aqueous solution at pH 7.4. Further analysis of their solution behavior has shown the observed luminescence intensity is significantly diminished below about pH $\sim$ 6 because of an apparent quenching mechanism involving protonation of the amine backbones. Nonetheless, under biologically relevant conditions, these complexes are promising candidates for applications in Homogeneous Time-Resolved Fluorescence (HTRF) assays and synthetic methodology to prepare derivatives with either a terminal amine or a carboxylate group suitable for bioconjugation has been developed. Lastly, we have demonstrated the use of these compounds as the energy donor in a Luminescence Resonance Energy Transfer (LRET) biological assay format.

Introduction

Recently, there have been several reports[1−3] on the use of luminescent Eu(III) and Tb(III) complexes for the detection of important biomolecules such as citrate, lactate, or urate in biological fluids. These assays utilize subtle changes in the characteristic lanthanide emission upon analyte binding, and offer both improved detection limits and allow for significantly smaller sample volumes to be used. Concurrently, Time-Resolved Luminescence Resonance Energy Transfer (TR-LRET) assays have continued to be developed,[4] enabling the convenient and sensitive high-throughput study of molecular interactions such as those occurring between proteins and their inhibitors.[5] In particular, the sharp emission spectra, large effective Stokes shifts, and long-lived luminescent lifetimes makes trivalent lanthanide cations such as Eu(III) very attractive, since the use of both spectral and time-resolved discrimination of the luminescent signal from background autofluorescence results in improved sensitivity.

We recently reported[6,7] on the exceptional luminescence properties of 1-hydroxypyridin-2-one (1,2-HOPO) based compounds as sensitizers for Eu(III), and our progress with these compounds was also summarized in a recent review.[8] Herein, we expand on our earlier communication[9] regarding the aqueous stability and photophysical properties of Eu(III) complexes with the tetradentate 5LIN^{Me}-1,2-HOPO and octadentate H(2,2)-1,2-HOPO ligands (Chart 1). We have found that protonation of the apical amines is important in determining the luminescence intensity and resulting photophysical properties for these complexes, and with the help of TD-DFT calculations, suggest a possible rationale for this effect. We also introduce two new functionalized octadentate derivatives which bear either a pendant amine or a carboxylate arm to enable conjugation of the complexes with relevant biomolecules. We have measured the stability and photophysical properties of these new compounds, and find they are essentially unchanged when compared to the parent complex. Lastly, we demonstrate the feasibility of using these complexes as a long-lived luminescent tag in a bioassay format, using a 1,2-HOPO labeled streptavidin bioconjugate

*To whom correspondence should be addressed. E-mail: raymond@socrates.berkeley.edu. Phone: +1 510 642 7219. Fax: +1 510 486 5283.

(1) Leonard, J. P.; dos Santos, C. M. G.; Plush, S. E.; McCabe, T.; Gunnlaugsson, T. *Chem. Commun.* **2007**, *2*, 129–131.
(2) Pal, R.; Parker, D.; Costello, L. C. *Org. Biomol. Chem.* **2009**, *7*, 1525–1528.
(3) Esplin, T. L., Cable, M. L., Gray, H. B., Ponce, A., *Inorg. Chem.* **2010**, *49*, 4643−4647.
(4) Vogel, K. W.; Vedvik, K. L. *J. Biomol. Screening* **2006**, *11*, 439–443.
(5) Bergendahl, V.; Heyduk, T.; Burgess, R. R. *Appl. Environ. Microbiol.* **2003**, *69*, 1492–1498.
(6) Moore, E. G.; Xu, J.; Jocher, C. J.; Werner, E. J.; Raymond, K. N. *J. Am. Chem. Soc.* **2006**, *128*, 10648–10649.
(7) Moore, E. G.; Xu, J.; Jocher, C. J.; Castro-Rodriguez, I.; Raymond, K. N. *Inorg. Chem.* **2008**, *47*, 3105–3118.
(8) Moore, E. G.; Samuel, A. P. S.; Raymond, K. N. *Acc. Chem. Res.* **2009**, *42*, 542–552.
(9) Moore, E. G.; Jocher, C. J.; Xu, J.; Werner, E. J.; Raymond, K. N. *Inorg. Chem.* **2007**, *46*, 5468–5470.

Published on Web 09/27/2010

Chart 1. Chemical Structures of Tetradentate and Octadentate 1,2-HOPO Based Ligands Discussed in This Paper

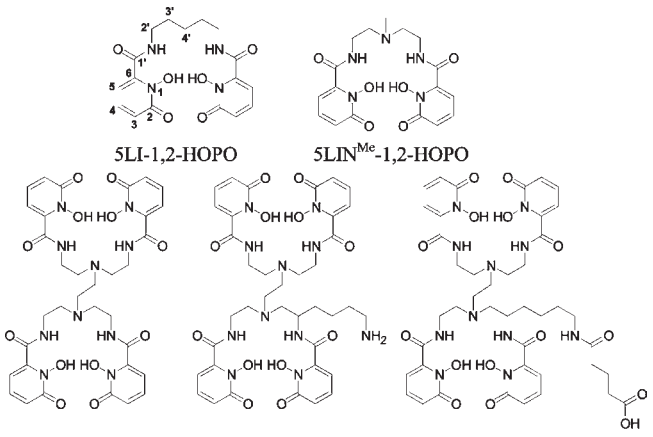

as the energy donor and a biotinylated organic dye, Alexa Fluor 594, as the energy acceptor.

Experimental Section

General Procedures. All solvents for reactions were dried using standard methodologies. Biocytin Alexa Fluor 594 was purchased from Invitrogen as the sodium salt and was used as supplied. Thin-layer chromotography (TLC) was performed using precoated Kieselgel 60 F254 plates. Flash chromatography was performed using EM Science Silica Gel 60 (230−400 mesh). NMR spectra were obtained using either Bruker AM-300 or DRX-500 spectrometers operating at 300 (75) MHz and 500 (125) MHz for ^{1}H (or ^{13}C) respectively. ^{1}H (or ^{13}C) chemical shifts are reported in parts per million (ppm) relative to the solvent resonances, taken as δ 7.26 (δ 77.0) and δ 2.49 (δ 39.5) for $CDCl_3$ and $(CD_3)_2SO$, respectively, while coupling constants (J) are reported in hertz (Hz). The following standard abbreviations are used for characterization of ^{1}H NMR signals: s = singlet, d = doublet, t = triplet, q = quartet, quin = quintet, m = multiplet, dd = doublet of doublets. Fast-atom bombardment mass spectra (FABMS) were performed using 3-nitrobenzyl alcohol (NBA) or thioglycerol/glycerol (TG/G) as the matrix. Elemental analyses were performed by the Microanalytical Laboratory, University of California, Berkeley, CA.

Synthesis. The detailed syntheses of 5LIN^{Me}-1,2-HOPO and H(2,2)-1,2-HOPO and their Eu(III) complexes have been previously reported,[9] as well as many of the relevant precursors (see Scheme 1) including the activated 1,2-HOPO-Bn-acid-chloride.[10] Aziridine was prepared from 2-aminoethyl hydrogen sulfate using literature methodologies.[11] Similarly, the synthesis of Cbz-Lys(Boc)-aldehyde and Benzyl Phenyl Carbonate have been reported elsewhere.[12,13]

Cbz-aziridine. The concentrations of aziridine in the freshly prepared distillate[11] were calibrated by acid−base titration and were found to range from 0.1 to 0.2 M, which was used directly for preparation of Cbz-aziridine. Hence, to a stirred solution of the distillate (500 mL, 0.1 mol) in a round-bottom flask with external cooling via an ice bath, 3 equiv of potassium carbonate were added. After all the solid had dissolved, benzyl choloroformate (1.5 equiv) in Et_2O (150 mL) was added over a 2 h period. The solution was stirred overnight, warmed to room temperature, and the aqueous phase was extracted with CH_2Cl_2 (5 × 30 mL). The organic phases were combined and passed through a flash silica gel pad, then concentrated to afford the desired Cbz-aziridine (7.2 g, 81%) as a thick, colorless oil. ^{1}H NMR (500 MHz, $CDCl_3$, 25 °C): δ = 2.22 (s, 4H, CH_2), 5.14 (s, 2H, CH_2), 7.34 (m, 5H, ArH). ^{13}C NMR (125 MHz, $CDCl_3$, 25 °C): δ = 20.51, 65.93, 127.3, 127.4, 128.7, 140.9, 159.4.

Cbz$_2$-TREN. Benzyl Phenyl Carbonate (4.56 g, 20 mmol) was added to a stirring solution of tris(ethylenediamine) (TREN, 1.46 g, 10 mmol) in absolute EtOH (50 mL) while cooling with an ice bath. The reaction mixture was stirred overnight at room temperature, and the volatiles were removed in vacuo. Distilled water (50 mL) was added to the oily residue, and the pH was adjusted to 3 by addition of aqueous HCl (2 M), again using an external ice bath for cooling. The acidified solution was extracted with CH_2Cl_2 (4 × 50 mL). The cooled aqueous phase was then made strongly alkaline by addition of aqueous NaOH (2 M) and extracted with CH_2Cl_2 (3 × 80 mL). The organic phase was dried over Na_2SO_4, filtered, and loaded onto a basic alumina column. Gradient chromatography with 3−6% CH_3OH in CH_2Cl_2 and then concentration afford pure Cbz$_2$-TREN (3.10 g, 75%) as a thick, colorless oil. ^{1}H NMR (500 MHz, $CDCl_3$, 25 °C): δ = 2.48 (t, 2H, J = 5.5 Hz, CH_2), 2.56 (s,br, 4H, CH_2), 2.67 (t, 2H, J = 5.5 Hz, CH_2), 3.23 (s,br, 4H, CH_2), 5.06 (s, 2H, CH_2), 5.72 (s, 2H, CbzNH), 7.04 (m, 10H, ArH). ^{13}C NMR (125 MHz, $CDCl_3$, 25 °C): δ = 38.9, 39.4, 53.8, 52.7, 66.3, 127.78, 127.82, 136.6, 156.7. MS (FAB, NBA) $C_{22}H_{30}N_4O_4$: $[M+H]^+$ 415.0.

Cbz$_2$-TREN-Cbz-Lys(Boc). Cbz$_2$-TREN (4.14 g, 10 mmol) and Cbz-Lys(Boc)-aldehyde (3.64 g, 10 mmol) were mixed in THF (50 mL) at room temperature under N_2. The mixture was stirred for 3 h, then sodium triacetoxyborohydride (3.18 g, 15 mmol) was added and the mixture stirred at room temperature under a N_2 atmosphere for 24 h. Aqueous NaOH (1 M) was added to quench the reaction mixture, and the mixture was extracted with CH_2Cl_2 (3 × 50 mL). The CH_2Cl_2 extract was loaded onto a flash silica gel column. The appropriate fractions of a gradient elution with 3−10% MeOH in CH_2Cl_2 were collected and evaporated to dryness to give the desired product (6.27 g, 82%) as a thick, pale beige oil. ^{1}H NMR (500 MHz, $CDCl_3$, 25 °C): δ = 1.17 (s,br, 2H, Lys CH_2), 1.24−1.89 (m, 4H, Lys CH_2), 1.41 (s, 9H, Boc CH_3), 2.53 (s, br, 8H, Tren CH_2), 3.03 (s, 2H, BocNHCH_2), 3.14 (s, 2H, CbzNHCH_2), 3.20 (s, 2H, CbzNHCH_2), 3.64 (s,br, 1H, Lysine chiral CH), 4.54 (s, 1H, BocNH), 5.05(m, 6H, CbzCH_2), 7.27 (m, 15H, ArH). ^{13}C NMR (125 MHz, $CDCl_3$, 25 °C): δ, 22.8, 28.3, 29.5, 32.5, 39.4, 39.9, 47.4, 50.9, 53.8, 54.3, 66.5, 78.9, 79.3, 127.9, 128.1, 128.4, 136.6, 156.0, 156.7, 156.9. MS (FAB, NBA) $C_{41}H_{58}N_6O_8$: $[M+H]^+$ 763.5.

Cbz$_4$-Lys-Boc-H(2,2)-amine. Cbz$_2$-TREN-Cbz-Lys(Boc) (3.81 g, 5 mmol) and Cbz-aziridine (1.24 g, 7 mmol) were mixed in *t*-butanol (50 mL) at room temperature under an N_2 atmosphere. The mixture was heated to 80 °C and stirred under N_2 for 16 h, when TLC showed the reaction was complete. The volatiles were removed under vacuum, and the residue was dissolved in CH_2Cl_2. The appropriate fractions of a gradient flash silica gel column (1−7% MeOH in CH_2Cl_2) were collected and evaporated to dryness to give the desired product as a thick, pale beige oil (3.98 g, 84.7%). ^{1}H NMR (500 MHz, $CDCl_3$, 25 °C): δ = 1.24−1.87 (m, 6H, Lys CH_2), 1.42 (s, 9H, Boc CH_3), 2.26 (s, br, 2H, CH_2), 2.47 (m,br,, 6H, CH_2), 2.58 (s,br, 2H, CH_2), 2.93−3.35 (m,br, 8H, CH_2), 5.05 (m, 8H, CbzCH_2), 7.27 (m, 20H, ArH). ^{13}C NMR (125 MHz, $CDCl_3$, 25 °C): δ 22.8, 28.4, 29.7, 31.2, 32.9, 38.5, 38.7, 40.1, 49.4, 52.1, 52.3, 59.4, 66.5, 69.1, 78.9, 127.9, 127.9, 128.0, 128.1, 128.36, 128.38, 136.57, 136.64, 156.0, 156.7. MS (FAB, NBA) $C_{51}H_{69}N_7O_{10}$: $[M+H]^+$ 940.5.

Boc-Lys-H(2,2)-amine. To a glass hydrogenation container with 200 mg of wet 5% Pd/C catalyst, 5 mL of MeOH was

(10) Xu, J.; Churchill, D. G.; Botta, M.; Raymond, K. N. *Inorg. Chem.* **2004**, *43*, 5492–5494.
(11) Reeves, W. A.; Drake, G. L., Jr.; Hoffpauir, C. L. *J. Am. Chem. Soc.* **1951**, *73*, 3522.
(12) McConnell, R. M.; Barnes, G. E.; Hoyng, C. F.; Gunnl, J. M. *J. Med. Chem.* **1990**, *33*, 86–93.
(13) Pittelkow, M.; Lewinsky, R.; Christensen, J. B. *Synthesis* **2002**, *15*, 2195–2202.

Scheme 1. Synthetic Scheme for Preparation of Functionalized Octadentate 1,2-HOPO Ligands

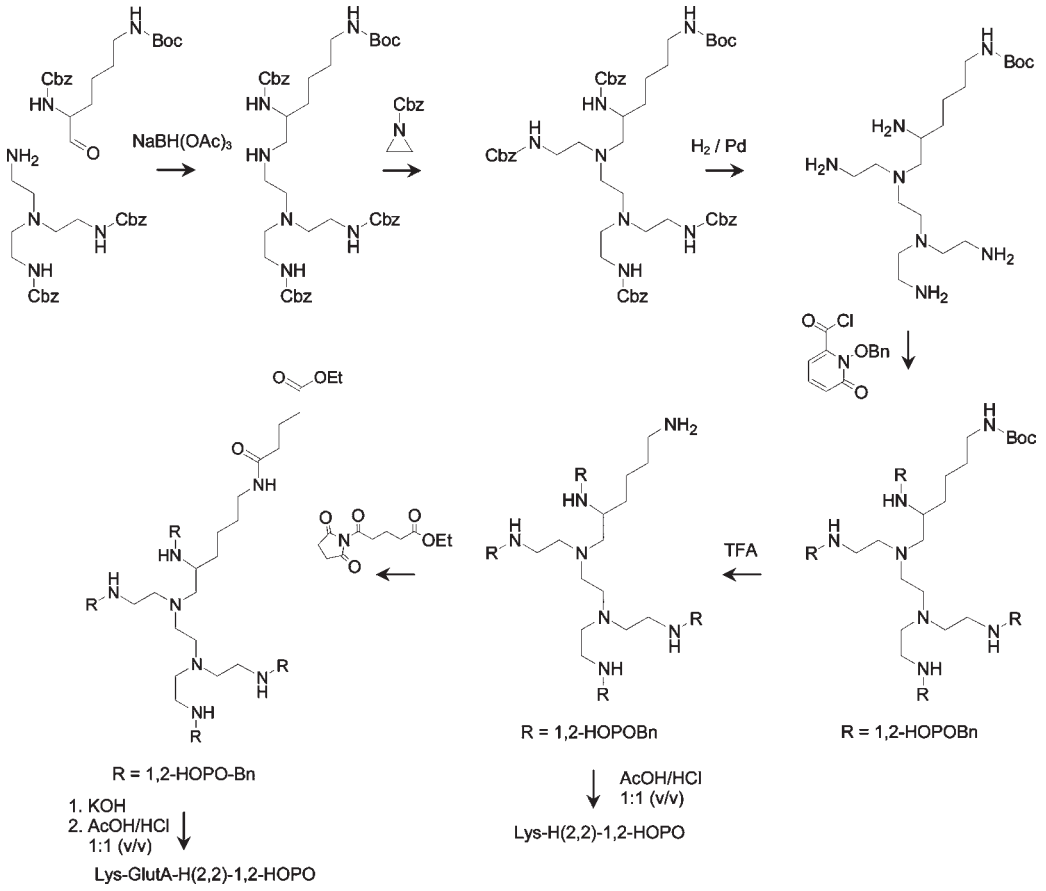

carefully added along the glass wall to cover the catalyst (***Caution! Pd/C catalyst is pyrophoric***). A solution of Cbz_4BocLys-H(2,2)-amine (0.94 g, 1 mmol) in MeOH (30 mL) was added to the container, which was placed in a Parr bomb apparatus and hydrogenated at 500 psi overnight. Subsequent TLC analysis confirmed the absence of starting material, and the solvent was removed in vacuo. The Boc-Lys-H(2,2)-amine was obtained as a colorless thick oil (0.52 g, 90%), isolated as the tetracarbonate form through reaction with atmospheric CO_2. The desired free amine form was prepared by passage of this product through a strongly basic ion exchange column. ^{1}H NMR (500 MHz, $CDCl_3$, 25 °C): δ = 1.24−1.87 (m, 6H, Lys CH_2), 1.42 (s, 9H, Boc CH_3), 2.41−2.82 (m, br, 10H, CH_2), 2.82−3.23 (m, br, 9H, CH_2), 3.29 (s, br, 1H, CH), 5.48(s, 1H, Boc NH), 8.52 (s, 3H, CarbonateNH). ^{13}C NMR (125 MHz, $CDCl_3$, 25 °C): δ 22.6, 28.4, 29.5, 31.1, 37.0, 39.9, 49.8, 51.9, 68.8, 78.6, 156.2, 169.0. MS (FAB, NBA) $C_{51}H_{69}N_7O_{10}$: $[M+H]^+$ 404.4.

Boc-Lys-H(2,2)-1,2-HOPO-Bn. To a freshly prepared solution of Boc-Lys-H(2,2)-amine (0.2 g, 0.5 mmol) in CH_2Cl_2 (20 mL), cooled with an ice bath and vigorously stirred, was added 2 mL of 40% K_2CO_3 solution. A solution of 1,2-HOPO-Bn-acid-chloride (freshly prepared from 0.75 g 1,2-HOPO-Bn acid, 3 mmol) in dichloromethane (20 mL) was added slowly via a Teflon tube equipped with a glass capillary tip over a period of 1 h. The reaction mixture was allowed to warm to room temperature and was stirred overnight, and then the mixture was washed with 1 M HCl (20 mL), then saline (20 mL), and was loaded onto a flash silica column. Elution with 2−8% MeOH in CH_2Cl_2 allows the separation of the benzyl-protected precursor Boc-Lys-H(2,2)-1,2-HOPO-Bn as a beige foam (0.46 g, 70%). ^{1}H NMR (300 MHz, DMSO-d_6, 25 °C): δ = 1.15 (s,br, 4H), 1.41 (s, 9H, BocH), 1.9−2.8 (m, 14H), 2.8−3.3 (m, 8H), 3.79 (s, br, 1H), 4.90−5.40 (m, 8H), 6.03 (s, 1H), 6.17 (d, 3H), 6.53 (d, 1H), 6.60 (d, 3H), 6.94 (d, 1H), 7.0−7.4 (m, 19H), 7.4−7.5 (m, 8H), 7.71 (s, 1H, NH). ^{13}C NMR (125 MHz, $CDCl_3$, 25 °C): δ = 22.8, 28.2, 29.3, 31.9, 37.4, 37.5, 39.8, 48.7, 51.5, 51.9, 52.8, 53.3, 53.7, 59.0, 78.6, 79.0, 104.6, 105.0, 123/1, 128.3, 129.1, 129.7, 129.9, 130.0, 133.2, 133.3, 137.9, 138.1, 142.9, 143.1, 155.9, 158.1, 158.2160.5, 160.7. MS (FAB, NBA) $C_{71}H_{81}N_{11}O_{14}$: $[M+H]^+$ 1312.0.

Lys-H(2,2)-1,2-HOPO. Boc-Lys-H(2,2)-1,2-HOPO-Bn (0.26 g, 0.2 mmol) was dissolved in a 1:1 (v/v) mixture of concentrated HCl (12 M) and glacial CH_3COOH (20 mL) and was stirred at room temperature for 2 days. Filtration followed by removal of the solvent gave the desired product as a beige solid (0.18 g, 81%). ^{1}H NMR (300 MHz, DMSO-d_6, 25 °C): δ = 1.2−1.7 (m, br, 6H), 2.74 (s, br, 3H), 3.05 (s, br, 3H), 3.15 (s, br, 5H), 3. 55 (s, br, 3H), 3.61 (s, br, 6H), 4.15 (s, br, 1H), 6.30−6.45 (m, 4H), 6.60 (d, 4H), 7.39 (m, 5H), 7.88 (s, br, 3H), 8.85 (s, br, 1H), 9.00 (s, br, 1H), 9.06 (s, br, 2H). MS (FAB, NBA): 851 $[M+H]^+$. Anal. for $C_{38}H_{49}N_{11}O_{12}\cdot 2HCl\cdot H_2O\cdot 2CH_3OH$ (1066.88 g·mol^{-1}), Calcd (Found): C, 47.72 (47.60); H, 6.11 (6.17); N, 15.30 (15.34).

Lys-EtGlutA-H(2,2)-1,2-HOPO-Bn. To a solution of Boc-Lys-H(2,2)-1,2-HOPO-Bn (0.26 g, 0.2 mmol) in 2 mL of CH_2Cl_2 cooled with an ice bath was added 2 mL of CF_3COOH. The mixture was stirred for 4 h then evaporated to dryness at room temperature, and TLC analysis confirmed removal of the Boc protecting group. The residue was dissolved in dry THF (20 mL), and dry Et_3N (0.5 mL) was added, cooling with an ice bath. To this cold mixture, an excess of ethyl glutarate *N*-hydroxy-succinimide ester (0.1 g, 0.4 mmol) was added under nitrogen. The mixture was stirred for 4 h, and the volatiles were removed in vacuo. The residue was dissolved in CH_2Cl_2 and loaded onto a flash silica column. Elution with 2−8% methanol in CH_2Cl_2 allows the separation of the benzyl-protected precursor Lys-EtGlutA-H(2,2)-1,2-HOPO-Bn as a beige foam (0.19 g, 70%).

^{1}H NMR (300 MHz, DMSO-d_6, 25 °C): δ = 1.09 (s, br, 4H), 1.20 (t, 3H), 1.25 (t, 4H), 1.84 (t, 2H), 2.02 (m, 2H), 2.17 (t, 6H), 2.28 (t, 6H), 2.98−3.1 (m, 8H), 3.78 (s, br, 1H), 4.05 (q, 2H), 5.10−5.40 (m, 8H), 6.03 (s, 1H), 6.16 (d, 3H), 6.45 (s, 1H), 6.51 (d, 1H), 6.58 (d, 3H), 7.15 (dd, 1H), 7.18−7.40 (m, 18H), 7.40−7.51 (m, 8H), 8.00 (s, 1H, NH). ^{13}C NMR (125 MHz, $CDCl_3$, 25 °C): δ = 14.4, 21.2, 23.2, 25.5, 28.9, 31.9, 33.7, 35.5, 37.7, 38.2, 39.0, 46.0, 49.1, 50.4, 52.1, 53.2, 54.5, 59.9, 60.6, 79.4, 105.1, 105.6, 123.3, 123.5, 128.8, 129.6, 130.3, 130.4, 130.6, 133.7, 133.8, 138.7, 143.4, 143.7, 143.8, 158.7, 158.8, 161.0, 161.2, 161.5, 173.0, 173.5. MS (FAB, NBA) 1354 $[M+H]^+$.

Lys-GlutA-H(2,2)-1,2-HOPO. The deprotection of Lys-EtGlutA-H(2,2)-1,2-HOPO-Bn was performed in two steps. The first step was saponification of the pendant ethyl ester, followed by deprotection of the four benzyl groups under strongly acidic condition as described for Lys-H(2,2)-1,2-HOPO-Bn. To a solution of Lys-EtGlutA-H(2,2)-1,2-HOPO-Bn (0.27 g, 0.2 mmol) in 5 mL of methanol, cooled with an ice bath, was added 2 mL of KOH solution (1 M). The mixture was stirred for 4 h when TLC confirmed the hydrolysis of the ethyl ester was complete. The mixture was evaporated to dryness at room temperature, and the residue was dissolved in water (10 mL). The hydrolyzed Lys-GlutA-H(2,2)-1,2-HOPO-Bn was precipitated upon acidification with HCl (1 M). This was collected, rinsed with cold water, and further deprotected by dissolving in a 1:1 (v/v) mixture of concentrated HCl (12 M) and glacial CH_3COOH (20 mL). After stirring at room temperature for 2 days, filtration followed by removal of the solvent gave the desired product as a beige solid (0.15 g, 71%). ^{1}H NMR (300 MHz, DMSO-d_6, 25 °C): δ = 1.37 (s, br, 4H), 1.67 (t, 7H), 1.84 (t, 2H), 2.03 (m, 2H), 2.17 (t, 6H), 2.28 (t, 6H), 2.98−3.1 (m, 8H), 3.78 (s, br, 1H), 4.05 (q, 2H), 6.41 (m, 4H), 6.60 (m, 4H), 7.39 (m, 4H), 7.78 (t, 1H), 8.83 (m, 1H), 8.80 (m, 1H), 9.05 (t, 2H). MS (FAB, NBA): 966.4 $[M+H]^+$. Anal. for $C_{43}H_{55}N_{11}O_{15}\cdot HCl\cdot 4H_2O$ (1074.48 g·mol^{-1}), Calcd (Found): C, 48.07 (48.34); H, 6.00 (6.09); N, 14.34 (14.00).

[Eu(Lys-H(2,2)-1,2-HOPO)]. To a solution of Lys-H(2,2)-1,2-HOPO (21.0 mg, 19.7 μmol) in MeOH (5 mL) was added 100 μL of pyridine, followed by 1.03 molar equivs of $EuCl_3\cdot 6H_2O$ (7.85 mg, 20.3 μmol) in MeOH (1 mL). The resulting mixture was refluxed for 4 h, then allowed to cool to room temperature. Addition of diethyl ether (ca. 10 mL) induced precipitation of a white solid, which was collected by vacuum filtration, washed with diethyl ether, and air-dried to yield the desired product (19.4 mg, 76.6%). Anal. for $EuC_{38}H_{45}N_{11}O_{12}\cdot 3HCl\cdot 2CH_3OH\cdot 6H_2O$ (1282.37 g·mol^{-1}), Calcd (Found): C, 37.46 (37.24); H, 5.42 (5.28); N, 12.01 (11.83).

[Eu(Lys-GlutA-H(2,2)-1,2-HOPO)]. This complex was prepared using the same methodology as the [Eu(Lys-H(2,2)-1,2-HOPO)] complex, substituting the Lys-GlutA-H(2,2)-1,2-HOPO ligand where appropriate (17.0 mg, 72.0%). Anal. for $EuC_{43}H_{52}N_{11}O_{15}\cdot HCl\cdot CH_3OH\cdot 5H_2O$ (1273.48 g·mol^{-1}), Calcd (Found): C, 41.50 (41.39); H, 5.30 (5.28); N, 12.10 (12.01).

SAv-[Eu(Lys-GlutA-H(2,2)-1,2-HOPO)]. Lys-GlutA-H(2,2)-1,2-HOPO (5.5 mg, 5.1 μmol) was dissolved with *N*-hydroxysulfosuccinimide (5.54 mg, 25.5 μmol) and 1-ethyl-3-(3-dimethylaminopropyl)carbodiimide (4.75 mg, 30.6 μmol) in 127 μL of dry DMF, and then stirred for 2 h. The activated Lys-GlutA-H(2,2)-1,2-HOPO-sNHS ester was then directly added dropwise to a solution of streptavidin (160 μM, 0.13 μmol) in 100 mM Na_2CO_3 buffer at pH 9 and allowed to stir overnight at room temperature. The SAv-Lys-GlutA-H(2,2)-1,2-HOPO was separated from any unreacted Lys-GlutA-H(2,2)-1,2-HOPO and buffer-exchanged into 0.1 M TRIS at pH 7.0 using a Penefsky gel filtration column.[14] $EuCl_3.6H_2O$ (2.8 mg, 7.7 μmol) dissolved in sodium citrate buffer was then added to the SAv-Lys-GlutA-H(2,2)-1,2-HOPO conjugate while stirring to form the metal complex. The A341/280 absorbance ratio for Eu-Lys-GlutA-H(2,2)-1,2-HOPO was determined experimentally to be 0.486. The A341/280 ratio and a molar extinction coefficient of 18,200 M^{-1} cm^{-1} for the parent Eu-H(2,2)-1,2-HOPO complex were used to estimate a labeling ratio of about 2.3 [Eu(Lys-GlutA-H(2,2)-1,2-HOPO)] molecules per streptavidin molecule.

Physical Methods. Solution Thermodynamics. The general procedure used to compare aqueous stabilities of the Eu(III) complexes herein was that of competition batch titration as described previously,[15,16] using diethylenetriaminepentaacetic acid (DTPA) as the known competitor. Briefly, varying volumes of standardized DTPA stock solution were added to an aqueous 0.1 M HEPES buffer solution (pH 7.4) containing 0.1 M KCl electrolyte, and a fixed amount of the appropriate ligand and Eu(III) cation in 1:1 stoichiometry was delivered by Eppendorf pipet. If necessary, the pH of the solutions was readjusted to 7.4 with HCl and/or KOH, and the solutions were diluted to identical volumes with additional 0.1 M HEPES buffer (pH 7.4) containing 0.1 M KCl. The initial concentrations of DTPA relative to the Eu(III) complex ranged from about 1:10 to 3000:1. After standing for 24 h to ensure thermodynamic equilibrium, the concentration of the remaining complexed ligand was evaluated by monitoring the Eu(III) emission spectrum after 330 nm excitation, using the integrated area of the luminescence spectra in the wavelength range between 570 and 710 nm and the spectra of the fully formed complexes in the absence of added DTPA competitor as a reference.

Photophysics. Typical sample concentrations for absorption and fluorescence measurements were about 10^{-5} to 10^{-6} M and 1.0 cm cells in quartz suprasil or equivalent were used. UV−visible absorption spectra were recorded on a Cary 300 double beam absorption spectrometer. Emission spectra were acquired on a HORIBA Jobin Yvon IBH FluoroLog-3 spectrofluorimeter. Spectra were reference corrected for both the excitation light source variation (lamp and grating) and the emission spectral response (detector and grating). Quantum yields were determined by the optically dilute method using the following equation;

$$\frac{\Phi_x}{\Phi_r} = \left[\frac{A_r(\lambda_r)}{A_x(\lambda_x)}\right]\left[\frac{I(\lambda_r)}{I(\lambda_x)}\right]\left[\frac{\eta_x^2}{\eta_r^2}\right]\left[\frac{D_x}{D_r}\right]$$

where A is the absorbance at the excitation wavelength (λ), I is the intensity of the excitation light at the same wavelength, η is the refractive index, and D is the integrated luminescence intensity. The subscripts "x" and "r" refer to the sample and reference, respectively. Quinine sulfate in 1.0 *N* sulfuric acid was used as the reference (Φ_r = 0.546).[17]

Luminescence lifetimes were determined with a HORIBA Jobin Yvon IBH FluoroLog-3 spectrofluorimeter, adapted for time-resolved measurements. A submicrosecond Xenon flash lamp (Jobin Yvon, 5000XeF) was used as the light source, coupled to a double grating excitation monochromator for spectral selection. The input pulse energy (100 nF discharge capacitance) was about 50 mJ, yielding an optical pulse duration of less than 300 ns at fwhm. A thermoelectrically cooled single photon detection module (HORIBA Jobin Yvon IBH, TBX-04-D) incorporating fast rise time PMT, wide bandwidth preamplifier and picosecond constant fraction discriminator was used as the detector. Signals were acquired using an IBH DataStation Hub photon counting module, and data analysis was performed using the commercially available DAS 6 decay analysis software package from HORIBA Jobin Yvon IBH. Goodness of fit was assessed by minimizing the reduced chi squared function, χ^2, and

(14) Penefsky, H. S. *Methods Enzymol.* **1979**, *56*, 527–530.

(15) Pierre, V. C.; Botta, M.; Aime, S.; Raymond, K. N. *Inorg. Chem.* **2006**, *45*, 8355–8364.

(16) Doble, D. M. J.; Melchior, M.; O'Sullivan, B.; Siering, C.; Xu, J.; Pierre, V. C.; Raymond, K. N. *Inorg. Chem.* **2003**, *42*, 4930–4937.

(17) Crosby, G. A. D., J. N. *J. Phys. Chem.* **1971**, *75*, 991–1024.

a visual inspection of the weighted residuals. Each trace contained at least 10,000 points, and the reported lifetime values result from at least three independent measurements.

Computational Studies. Ground state density functional theory (DFT) and time-dependent DFT (TD-DFT) calculations were performed at the Molecular Graphics and Computational Facility, College of Chemistry, University of California, Berkeley. In both cases, the B3LYP/6-311G++ (d,p) basis set provided in Gaussian'03[18] was used, with simplified input structures derived from a previously reported[7] crystal structure. All calculations were done in the gas phase and geometry optimizations were performed with no symmetry restraints.

Results and Discussion

Synthesis. The synthesis of the 5LIN^{Me}-1,2-HOPO and H(2,2)-1,2-HOPO ligands were reported earlier,[9] and rely on an amide coupling reaction between primary amines of the ligand backbone and benzyl protected 1,2-HOPO carboxylic acid, activated by conversion to the acid chloride. Adopting similar methodologies, the synthetic route toward the new pivotal building block, Lys-H(2,2)-amine, is illustrated in Scheme 1 and has also been detailed in a recent patent.[19] The selective Cbz protection of TREN to yield Cbz_2-TREN, and subsequent Schiff base condensation product with Cbz-Lys(Boc)-aldehyde, obtained using literature procedures,[12] leads to Cbz_2-TREN-Cbz-Lys(Boc) after in situ reduction with $NaBH(OAc)_3$. This intermediate can be coupled in good yield with the highly reactive Cbz-aziridine to give the Cbz_4-Lys-Boc-H(2,2)-amine, which after catalytic hydrogenation and purification by cation exchange chromatography, yields the monoprotected Boc-Lys-H(2,2)-amine. Standard coupling procedures with the aforementioned benzyl protected 1,2-HOPO acid chloride yields Boc-Lys-H(2,2)-1,2-HOPO-Bn, which after strongly acidic deprotection using 1:1 (v/v) conc. HCl/AcOH yields the desired amine functionalized Lys-H(2,2)-1,2-HOPO chelate. Alternately, selective deprotection of the Boc group using TFA affords Lys-H(2,2)-1,2-HOPO-Bn which can be coupled with activated ethyl glutarate *N*-hydroxysuccinimide ester to give Lys-EtGlutA-H(2,2)-1,2-HOPO-Bn. Subsequent stepwise saponification of the ethyl ester under basic conditions and then removal of the benzyl protecting groups under strong acidic conditions gives the carboxylate functionalized Lys-GlutA-H(2,2)-1,2-HOPO chelate.

The complexation of either the 5LIN^{Me}-1,2-HOPO or H(2,2)-1,2-HOPO ligands with $EuCl_3 \cdot 6H_2O$ is readily achieved using the appropriate 1:2 or 1:1 metal/ligand stoichiometries respectively in the presence of pyridine acting as a base, and using MeOH as the solvent. After a short reflux period of about 4−6 h, the desired complexes were isolated upon cooling by filtration in excellent yield and in analytically pure form. Similarly, the complexation reactions of the new octadentate H(2,2)-ligands bearing amine or carboxylate functional groups were straightforward, and yielded the desired complexes as the protonated trihydrochloride and monohydrochloride salts, respectively, because of the differing protonation state of the terminal functional group (i.e., $-NH_3^+$ versus $-COO^-$, respectively).

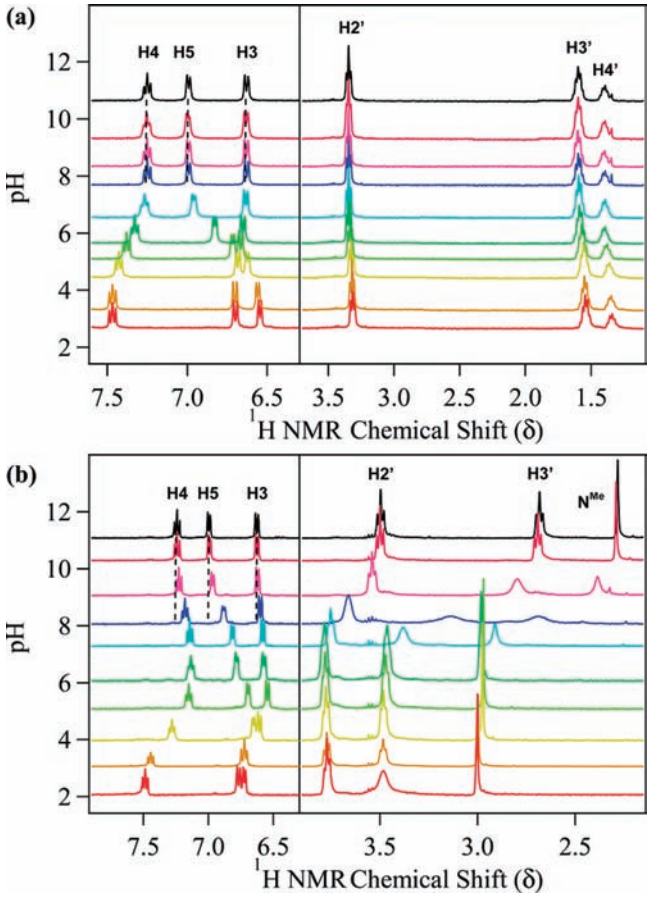

Figure 1. ^{1}H NMR spectra at various pH values (left axis intercept) for (**a**) the 5LI-1,2-HOPO (top) and (**b**) 5LIN^{Me}-1,2-HOPO (bottom) ligands.

Solution Thermodynamics. The protonation constants for the tetradentate 5LIN^{Me}-1,2-HOPO and octadentate H(2,2)-1,2-HOPO ligands, as determined by potentiometric titration, were detailed earlier, together with the experimental pEu values and calculated formation constants with Eu(III).[9] However, to gain further insight into the solution behavior, we have conducted additional ^{1}H NMR titrations for the ligand, in comparison to the structurally analogous tetradentate 5LI-1,2-HOPO ligand, which lacks an alkyl amine in the backbone. As a result, the previously assigned pK_a at 8.13, which we attributed to the amine, can be unequivocally confirmed by the observed shift in the *N*-methyl group resonance from about 2.2 ppm (basic) to about 3.0 ppm (acidic) between pH 10 to pH 6 (Figure 1b), consistent with an increase in deshielding of this resonance by the adjacent

(18) Frisch, M. J., Trucks, G. W., Schlegel, H. B., Scuseria, G. E., Robb; M. A., C., J. R., Montgomery, J. A., Jr., Vreven, T.; Kudin; K. N., B., J. C., Millam, J. M., Iyengar, S. S., Tomasi, J., Barone; V., M., B., Cossi, M., Scalmani, G., Rega, N., Petersson, G. A.; Nakatsuji, H., Hada, M., Ehara, M., Toyota, K., Fukuda, R., Hasegawa; J., I., M., Nakajima, T., Honda, Y., Kitao, O., Nakai, H., Klene; M., L., X., Knox, J. E., Hratchian, H. P., Cross, J. B., Bakken, V.; Adamo, C., Jaramillo, J., Gomperts, R., Stratmann, R. E., Yazyev; O., A., A. J., Cammi, R., Pomelli, C., Ochterski, J. W., Ayala; P. Y., M., K., Voth, G. A., Salvador, P., Dannenberg, J. J.; Zakrzewski, V. G., Dapprich, S., Daniels, A. D., Strain, M. C., Farkas; O., M., D. K., Rabuck, A. D., Raghavachari, K., Foresman, J. B.; Ortiz, J. V., Cui, Q., Baboul, A. G., Clifford, S., Cioslowski, J.; Stefanov, B. B., Liu, G., Liashenko, A., Piskorz, P., Komaromi, I.; Martin, R. L., Fox, D. J., Keith, T., Al-Laham, M. A., Peng, C. Y.; Nanayakkara, A., Challacombe, M., Gill, P. M. W., Johnson, B., Chen; W., W., M. W., Gonzalez, C., Pople, J. A. *Gaussian 03*, revision C.02; Gaussian, Inc.: Wallingford, CT. 2004.

(19) Raymond, K. N.; Corneillie, T. M.; Xu, J. Luminescent hydroxyisophthalamide macrocyclic lanthanide complexes and derivatives. U.S. Patent 2007-US76047 2008063721, 20070815, 2008.

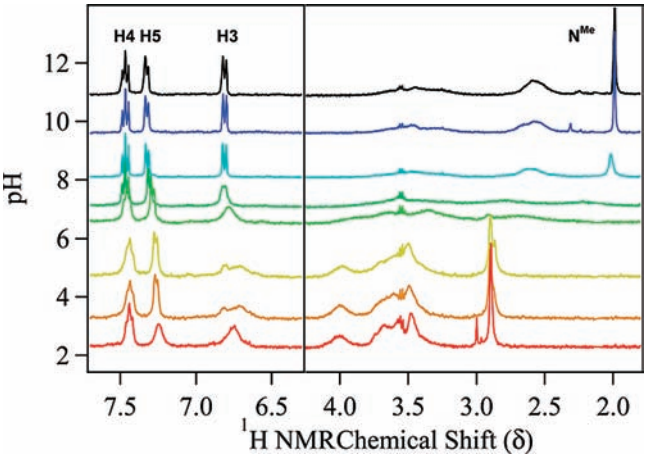

Figure 2. ^{1}H NMR spectra at various pH values (left axis intercept) for $[Y^{III}(5LIN^{Me}\text{-}1,2\text{-}HOPO)_2]$.

Chart 2. Structural Changes Associated with Protonation of the Tertiary Amine Group in $5LIN^{Me}$-1,2-HOPO

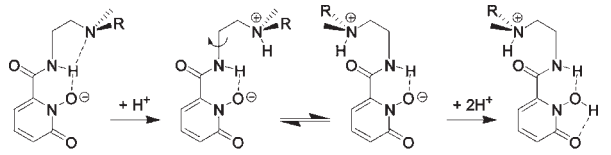

positive charge upon protonation. As previously assigned[20] using HMBC and HMQC 2D NMR techniques, we attribute the peaks at 6.62, 7.24, and 6.99 ppm (pH ~11) to the H3, H4, and H5 aromatic protons, respectively (Chart 1). Notably, concomitant with the spectral changes observed in the alkyl region was a slight upfield shift of these aromatic signals by 0.05, 0.1, and 0.18 ppm, respectively, (see dotted lines, Figure 1b) upon protonation of the amine backbone going from pH 10 to pH 6, which were not evident in the case of 5LI-1,2-HOPO. Since adjacent protonation should induce a downfield shift, this cannot be due to an inductive effect. As was the case for a related hexadentate ligand (Tren-1,2-HOPO),[20] we assign these shifts to a conformational change involving single bond rotation within the ligand backbone, facilitating intramolecular H-bonding interactions between the protonated amine and the amide carbonyl group(s), as shown in Chart 2. Further acidification beyond about pH 6 results in formation of the fully protonated $5LIN^{Me}$-1,2-HOPO ligand, and a corresponding downfield shift for the aromatic H3 and H4 signals. The observation of the sequential protonation equilibria for the equivalent *N*-hydroxyl groups was not possible by ^{1}H NMR, presumably because of their fast exchange on the NMR time scale.

The measured ^{1}H NMR spectra of the corresponding $[Eu(5LIN^{Me}\text{-}1,2\text{-}HOPO)_2]$ complex was very broad because of the paramagnetic nature of the metal ion and could not be interpreted. To further elucidate the solution behavior of this complex, we have substituted the lanthanide cation with Y(III), since this metal has an identical charge and very similar ionic radius[21] to Eu(III), but is diamagnetic. Consistent with our initial reports, the initial two protonation equilibria for the Y(III) complex can be readily assigned to protonation of the two amine backbones in the $[EuL_2]^-$ complex to form $[EuL_2H_2]^+$, since the apparent pK_a's of 7.5 and 6.5 determined by potentiometry correlate well with the observed shift of the *N*-methyl proton resonance from about 2.0 to 2.8 ppm between pH 8.1 and 4.7 (i.e., within ±1.5 pK_a units; Figure 2). The remaining pK_a at 4.5 has been assigned to protonation of one of the 1,2-HOPO chelate groups, most likely at an exposed keto oxygen atom, and is accompanied by a general broadening of the observed ^{1}H NMR spectra and a slight upfield shift of the resonances in the aromatic region, presumably because of the weaker electrostatic interaction and hence altered ligand exchange kinetics in going from an overall monocationic $[EuL_2H_2]^+$ complex involving two anionic ligands to the dicationic $[EuL_2H_3]^{2+}$ complex involving one anionic and one neutral ligand. Unfortunately, because of only limited solubility in aqueous solution (< 0.1 mM), the pH dependent ^{1}H NMR titration data could not be obtained for the H(2,2)-1,2-HOPO ligand, nor its Eu(III) or Y(III) complexes.

Having confirmed the protonation equilibria of complexes with 5LI-1,2-HOPO and $5LIN^{Me}$-1,2-HOPO, we were interested in the pH dependent behavior of the observed Eu(III) luminescence, and as such have undertaken fluorescence titrations at variable pH, with resulting data for 10 μM solutions of the bis(tetradentate) complexes as shown in Figure 3. When viewed together with the calculated speciation from the thermodynamic parameters, some striking features are seen. For the $[Eu(5LI\text{-}1,2\text{-}HOPO)_2]$ complex, the luminescence intensity is essentially constant across a wide pH range from 10 to 6, consistent with the expected speciation for the EuL_2 complex. Below pH 6, the concomitant formation of EuL_2H and, more importantly, hydrolysis of the EuL_2 complex to form $EuL(H_2O)_x$ contribute significantly to the speciation. Since the latter will have much weaker luminescence because of the well-known quenching effect of inner sphere water molecules,[22] this results in a decrease in the overall luminescence intensity. In stark contrast, the overall luminescence intensity of $[Eu(5LIN^{Me}\text{-}1,2\text{-}HOPO)_2]$ rapidly diminishes below pH 10 to about 50% of its maximum intensity at pH 7, which correlates to maximum formation of the $[EuL_2H]$ complex. Upon further acidification, the formation of $[EuL_2H_2]^+$ becomes dominant at about pH 5.8, and with the loss of the $[EuL_2]^-$ and $[EuL_2H]$ species, the luminescence is effectively switched off. Evidently, protonation of the amine backbones has a dramatic influence on the ensuing photophysical properties for the $[Eu(5LIN^{Me}\text{-}1,2\text{-}HOPO)_2]$ complex.

Although ^{1}H NMR data could not be obtained, data from fluorescence titrations that utilize significantly lower concentrations could be obtained for a 1 μM solution of [Eu(H(2,2)-1,2-HOPO)], and the corresponding luminescence intensities at variable pH for this complex are shown in Figure 3, together with the calculated speciation

(20) Jocher, C. J.; Moore, E. G.; Xu, J.; Avedano, S.; Botta, M.; Aime, S.; Raymond, K. N. *Inorg. Chem.* **2007**, *46*, 9182–9191.
(21) Shannon, R. D. *Acta Crystallogr.* **1976**, *A32*, 751–767.
(22) Beeby, A.; Clarkson, I. M.; Dickins, R. S.; Faulkner, S.; Parker, D.; Royle, L.; de Sousa, A. S.; Williams, J. A. G.; Woods, M. *J. Chem. Soc., Perkin Trans.* **1999**, 493–503.

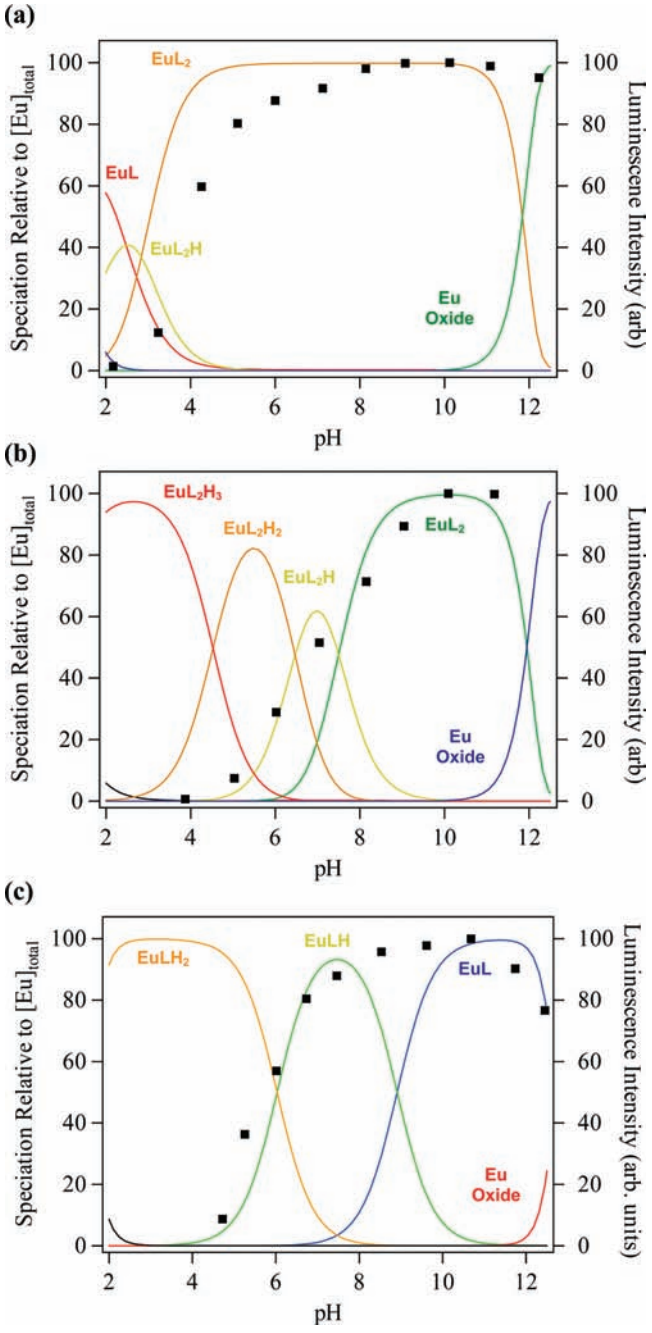

Figure 3. Combined pH dependent total integrated luminescence intensity profiles (right axis) (λ_{ex} = 330 nm, λ_{em} = 520−720 nm) in aqueous solution with expected speciation (left axis) from solution thermodynamic data for about 10 μM solutions of Eu(III) complexes with (**a**) 5LI-1,2-HOPO (top), (**b**) 5LIN^{Me}-1,2-HOPO (middle), and for a about 1 μM solution of the Eu(III) complex with (**c**) H(2,2)-1,2-HOPO (bottom).

obtained from the solution thermodynamic model. For this complex, given a tolerance of 1% free Eu(III), we previously reported[9] a calculated theoretical limit of stability of 5×10^{-17} M at pH 7.4. Upon re-examining this calculation, we noted that hydrolysis constants for the lanthanide cation were omitted, and the reported stability constants do not accurately reproduce the experimentally determined pEu values when these values are included. As such, the corrected values are reported here to be β_{110} = 22.3(1), β_{111} = 31.2(1), and β_{112} = 37.3(1). Nonetheless, because of a slight improvement in

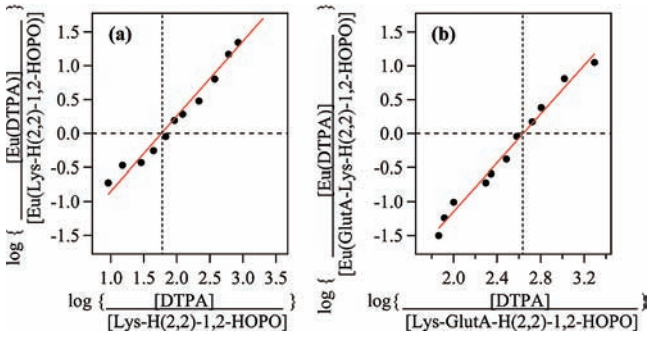

Figure 4. Double log plots of equilibrium Eu(III) complex concentrations determined from luminescence spectra versus equilibrium concentrations for (**a**) the Lys-H(2,2)-1,2-HOPO (left) and (**b**) Lys-GlutA-H(2,2)-1,2-HOPO (right) ligands. Solid lines are corresponding fits used to evaluate ΔpM versus Eu(DTPA), corresponding to pEu's of 20.7(1) and 21.8(4), respectively.

β_{110} when these constants are included, we still obtain a theoretical dilution limit with a similar order of magnitude of 1.6×10^{-16} M at pH 7.4 under the same tolerance condition of 1% free Eu(III), compared to 7×10^{-9} M for the [Eu(5LIN^{Me}-1,2-HOPO)$_2$] complex, with the exceptional resistance to hydrolysis being driven by the entropic chelate effect of the octadentate versus bis-(tetradentate) complex topologies.

As was the case for the tetradentate ligands, we note the luminescence at variable pH has a maximum intensity at about pH 10, which correlates well with the calculated speciation of the EuL complex. Upon acidification, the luminescence is again diminished, although the decrease is not as significant as was the case with the 5LIN^{Me}-1,2-HOPO ligand, amounting to only a about 13% decrease at pH 7.4 where the calculated [EuLH] speciation is at a maximum. Below about pH 6, where the formation of the $[EuLH_2]^+$ complex becomes dominant, we note the same dramatic decrease in overall Eu(III) based luminescence, again suggesting that protonation of the amine backbones effectively switches off luminescence from the metal center. Although the mechanism of this quenching is not readily apparent, it is most likely due to disruption of the overall sensitization process, as evidenced by our computational results (vide infra).

Despite this decrease in luminescence intensity at low pH, we note the H(2,2)-1,2-HOPO complex with Eu(III) still retains about 87% of its maximum luminescence at a biologically relevant pH of 7.4. As such, we carried on with the preparation of the Eu(III) complexes of the Lys-H(2,2)-1,2-HOPO and Lys-GlutA-H(2,2)-1,2-HOPO ligands, bearing pendant amine and carboxyl groups, respectively, and have assessed their aqueous stability at pH 7.4 by competition batch titration using DTPA as a known competitor (pEu ~ 19.04), with results as shown in Figure 4. The addition of increasing equivalents of DTPA results in the steady decrease of the characteristic Eu(III) luminescence for both the [Eu(Lys-H(2,2)-1,2-HOPO)] and the [Eu(Lys-GlutA-H(2,2)-1,2-HOPO)] complexes. From the accompanying double log plots, the point at which speciation between the ligand and DTPA is equivalent can be easily determined, and from the x intercept, the calculated pEu's for each complex at pH 7.4 were evaluated to be 20.7(1) and 21.8(4) with the Lys-H(2,2)-1,2-HOPO and Lys-GlutA-H(2,2)-1,2-HOPO ligands,

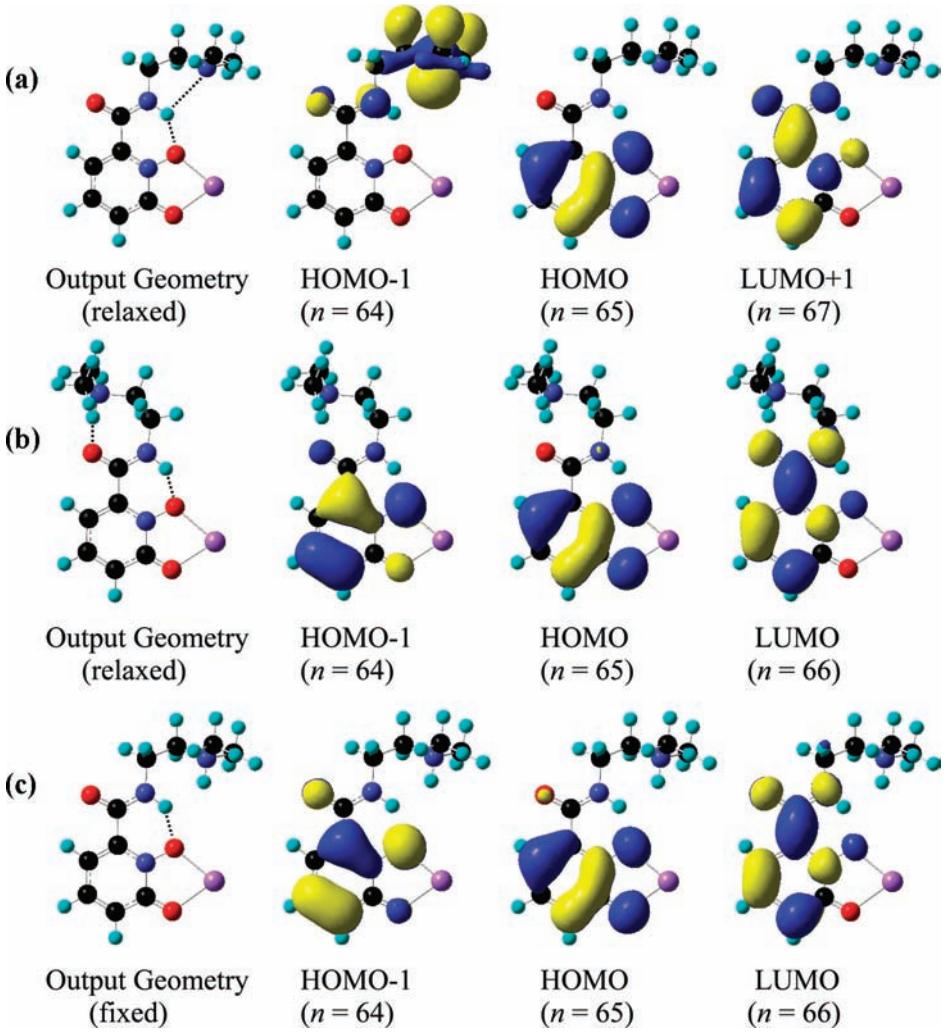

Figure 5. Calculated output geometries obtained from static B3LYP/6-311G^{+2}(d,p) geometry optimization and relevant molecular orbital diagrams from TD-DFT electronic structure calculations for (**a**) deprotonated [Na(Me_2N-Et-NHC(O)-1,2-HOPO)] (top), (**b**) protonated [Na(Me_2N^+H-Et-NHC(O)-1,2-HOPO)] (middle), and (**c**) protonated [Na(Me_2N^+H-Et-NHC(O)-1,2-HOPO)] (bottom) with "fixed" input geometry (see text).

respectively. These values are very similar to the previously reported pEu of 21.2 (1) at pH 7.4 for the unsubstituted [Eu(H(2,2)-1,2-HOPO)], and are also in accord with our earlier studies[23] of hexadentate HOPO chelates with Gd(III), where we noted that the overall complex charge can influence the ensuing aqueous stability.

Electronic Structure Calculations. In an effort to rationalize the mechanism for the quenching of Eu(III) centered luminescence after protonation of the adjacent amine backbones, TD-DFT calculations were applied to several simplified model systems. In accordance with strategies originally adopted[24] by Picard et al. and our own more recent reports,[25,26] we have replaced the trivalent lanthanide with monovalent sodium to avoid computationally expensive calculations involving the 4f metal. Although this is a crude model, we have found this approach to be useful and generally applicable in several cases as a tool for understanding the electronic structure of the lowest excited singlet and triplet states of the ligand.[27]

Hence, the model system as shown in Figure 5a was considered, which features a tertiary amine, separated by an ethyl chain from the 1,2-HOPO amide linkage, and this molecular fragment was first geometry optimized with no symmetry constraints, with the resulting output geometry as shown. Upon inspection, we note that the 1,2-HOPO motif including the amide group attachment is essentially planar, and the short C−O bond length of about 1.26 Å for the coordinated oxygen atom supports the keto resonance form. A symmetrical bidentate coordination mode with the monovalent sodium cation is apparent, with almost identical bond lengths of about 2.16 Å, mirroring that expected upon complexation with a trivalent lanthanide cation. The protons of the pendent ethyl chain between the amide nitrogen atom and the amine are staggered, although the amine and the amide nitrogen atoms have adopted a gauche conformation,

(23) Pierre, V. C.; Botta, M.; Aime, S.; Raymond, K. N. *Inorg. Chem.* **2006**, *45*, 8355–8364.
(24) Gutierrez, F.; Tedeschi, C.; Maron, L.; Daudey, J.-P.; Azema, J.; Tisnes, P.; Picard, C.; Poteau, R. *THEOCHEM* **2005**, *756*, 151–162.
(25) Moore, E. G.; Xu, J.; Jocher, C. J.; Castro Rodriguez, I.; Raymond, K. N. *Inorg. Chem.* **2008**, *47*, 3105–3118.
(26) Moore, E. G.; Xu, J.; Dodani, S. C.; Jocher, C. J.; D'Aleo, A.; Seitz, M.; Raymond, K. N. *Inorg. Chem.* **2010**, *49*, 4156–4166.
(27) Samuel, A. P. S.; Xu, J.; Raymond, K. N. *Inorg. Chem.* **2009**, *48*, 687–698.

Table 1. Summary of Electronic Structure Calculations for Deprotonated [Na(Me_2N-Et-NHC(O)-1,2-HOPO)] and Protonated [Na(Me_2N^+H-Et-NHC(O)-1,2-HOPO)] Model Complexes

excited state	multiplicity	energy (eV)	wavelength (nm)	oscillator strength	orbital(s) involved $n \rightarrow n'$	transition coefficient
			[Na(Me_2N-Et-NHC(O)-1,2-HOPO)] (Relaxed Geometry)			
1	T_1	2.620	473.3 ($\sim$ 21,130 cm^{-1})	0.0000	65 → 67 (HOMO→LUMO+1)	0.7628
2	T_2	3.175	390.6	0.0000	65 → 66	0.7028
3	S_1	3.192	388.4	0.0055	65 → 66	0.7035
4	T_3	3.216	385.5	0.0000	62 → 67	0.1182
					63 → 67	0.6656
					65 → 71	0.3681
5	S_2	3.719	333.4	0.1167	63 → 71	0.1523
					65 → 67	0.6357
			[Na(Me_2N^+H-Et-NHC(O)-1,2-HOPO)] (Relaxed Geometry)			
1	T_1	2.172	570.9 ($\sim$ 17,516 cm^{-1})	0.0000	65 → 66 (HOMO → LUMO)	0.7758
2	T_2	3.147	394.0	0.0000	64 → 66	0.7071
					64 → 69	0.1056
					65 → 69	0.2730
3	S_1	3.261	380.2	0.0872	64 → 69	0.1244
					65 → 66	0.6383
4	T_3	3.749	330.7	0.0000	64 → 66	−0.2431
					65 → 68	0.1403
					65 → 69	0.6529
5	T_4	3.845	322.4	0.0000	65 → 67	0.6939
			[Na(Me_2N^+H-Et-NHC(O)-1,2-HOPO (Fixed Geometry)			
1	T_1	2.462	503.6 ($\sim$ 19,860 cm^{-1})	0.0000	65 → 66 (HOMO → LUMO)	0.7428
					65 → 67	0.1184
					65 → 68	0.1146
2	T_2	2.618	473.7	0.0000	65 → 67	0.6890
					65 → 66	0.1327
3	S_1	2.640	469.6	0.0029	65 → 67	0.6993
4	T_3	3.272	379.0	0.0000	64 → 66	0.6695
					64 → 68	−0.1349
					65 → 74	0.3240
5	S_2	3.568	347.5	0.1102	64 → 74	−0.1256
					65 → 66	0.6400

rather than the more stable anti configuration. This is stabilized by a weak intramolecular H-bonding interaction between the amine lone pair and the amide proton, with a separation of about 2.66 Å. The amide proton is similarly involved in a much stronger intramolecular H-bonding interaction with the enolate oxygen atom, with a separation of about 1.78 Å.

The corresponding electronic structure calculation as determined by TD-DFT techniques using the same basis set is summarized in Table 1, and relevant molecular orbitals involved in these transitions are also depicted in Figure 5a. Most importantly, the lowest energy triplet state is predicted to occur at about 21,130 cm^{-1}, which is almost identical to the value of about 21,365 cm^{-1} previously calculated[25] for the Na^+ complex of a simpler 6-MeAmide-1,2-HOPO model system using the same TD-DFT techniques. Evidently, the presence of the ethyl amine chain has little influence over the electronic structure of the model systems when deprotonated.

Using the ground state optimized geometry for the deprotonated system as a starting point, but including an additional proton at the tertiary amine, we have performed a second geometry relaxation with the resulting output geometry as shown in Figure 5b. While the 1,2-HOPO motif and attached amide group are once again essentially planar as expected, the most significant difference, readily apparent on inspection, is a change in the $-C(O)-NH-CH_2-CH_2-$ bond torsion from −153° to +66°. As a consequence of the rotation of this bond, the ethyl amine substituent has adopted a gauche rather than anti conformation, and the proton of the amine group is directed toward the amide carbonyl, forming a very strong intramolecular H-bonding contact of about 1.55 Å. This change in conformation is reminiscent of that observed for the $5LIN^{Me}$-1,2-HOPO ligand at low pH, as monitored by ^{1}H NMR spectroscopy. Furthermore, since the amide NH proton is no longer involved in a bifurcated interaction with the tertiary amine lone pair, the strength of the H-bond between this group and the enolate oxygen atom is increased, as evidenced by a decrease in the intramolecular separation from about 1.78 to 1.65 Å, and the corresponding distance from the enolate oxygen to chelated metal cation is slightly elongated from about 2.15 to 2.22 Å.

The consequences of these changes in geometry on the electronic structure of the 1,2-HOPO chromophore subsequent to amine protonation were similarly assessed by TD-DFT techniques, with resulting lowest energy transitions as summarized in Table 1, and relevant molecular orbitals as depicted in Figure 5b. Clearly, the lowest energy triplet state is largely affected, with a significant decrease in the predicted energy of this transition from about 21,130 cm^{-1} to 17,516 cm^{-1}. Also apparent is a change in the nature of the HOMO-1 orbital from essentially an amine based lone pair in the former case to a π type orbital in the latter. As a result of the about 3600 cm^{-1} decrease in energy for the lowest energy triplet state (typically considered as the donor in the so-called "antennae" effect), the position of this level is about 1500 cm^{-1}

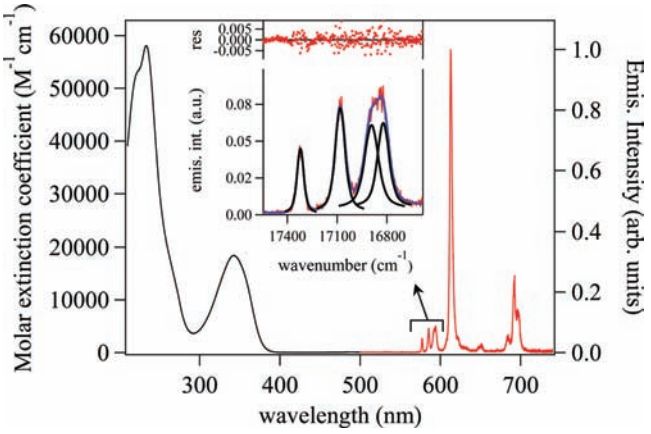

Figure 6. Absorption spectrum (black, left axis) and emission spectra at λ_{ex} = 330 nm (red, right axis) for [Eu(Lys-H(2,2)-1,2-HOPO)] in 0.1 M TRIS buffered aqueous solution at pH 7.4. Inset: Expansion of [Eu(Lys-H(2,2)-1,2-HOPO)] emission showing $^5D_0 \rightarrow {}^7F_0$ and $^5D_0 \rightarrow {}^7F_1$ transitions (red), and corresponding fit (blue) to four Voigt functions (black).

below the $^5D_1$ excited state, and only 239 cm^{-1} above the emitting $^5D_0$ level of the Eu(III) cation. In this region, the effects of thermal back energy transfer will be very significant, since the optimum energy separation for efficient energy transfer has been previously suggested to be at least about 1850 cm^{-1} above the emitting level of the Ln(III) cation.[28] This important result may explain the loss of luminescence intensity upon protonation of the amine backbones as observed by pH dependent fluorescence titrations.

Lastly, although molecular modeling at the MM2 level of theory for both the [Eu(5LIN^{Me}-1,2-HOPO)$_2$] and the [Eu(H(2,2)-1,2-HOPO)(H$_2$O)] complexes have shown that rotation of the ligand backbones (at least in part) is feasible (see Supporting Information, Figure S1), it could be argued that the extent of "protonation induced" amide rotation in the Eu(III) complexes is more conformationally restricted. To address this possibility, we have undertaken a third TD-DFT electronic structure calculation utilizing the fixed output geometry derived from the deprotonated amine case, but with the addition of a single proton to the tertiary amine nitrogen. As summarized in Table 1, the predicted energy of the lowest energy triplet state is once again reduced, from about 21,130 cm^{-1} to 19,860 cm^{-1}, although the decrease of 1270 cm^{-1} is not as dramatic. Nonetheless, even in this case, the location of this critical sensitizing level is only 830 cm^{-1} above the $^5D_1$ excited state of the Eu(III) cation, which is sufficiently close to facilitate efficient back energy transfer. Indeed, it has been shown previously that, based on selection rules for the direct energy transfer process, direct energy transfer to the $^5D_0$ level is not allowed, and it is likely the intermediate $^5D_1$ state which is the primary accepting level for energy transfer into the Eu(III) excited state manifold.[29]

Photophysics. The absorption spectra of the [Eu(5LIN^{Me}-1,2-HOPO)$_2$] and [Eu(H(2,2)-1,2-HOPO)] complexes were detailed in the preceding communication,[9] and the spectra of the new octadentate derivatives reported herein featuring either pendant amine or carboxylate arms are essentially identical when compared with the parent H(2,2)-1,2-HOPO complex. The UV−visible spectrum of [Eu(Lys-H(2,2)-1,2-HOPO)] is shown as an example in Figure 6. A broad electronic envelope assigned to n-π^* transitions of the 1,2-HOPO chromophore is evident, with peak maxima at about 342 nm, and at higher energy, a more intense band assigned to $\pi-\pi^*$ transitions of the chromophore is observed at about 233 nm.

The emission spectrum of the [Eu(Lys-H(2,2)-1,2-HOPO)] complex is also shown in Figure 6, and is characteristic of metal centered Eu(III) luminescence, with sharp bands attributable to the $^5D_0 \rightarrow {}^7F_J$ (J = 0, 1, 2, 3, and 4) transitions readily apparent at about 577, 585−597, 612, 650, and 680−700 nm. Notably, the splitting of the J = 1 transition into 3 peaks (see inset, Figure 6) is typical of that for the Eu(III) cation in a low-symmetry environment, and is consistent with our previous assignment[9] of local C_2 symmetry for the parent complex. The spectrum of the corresponding [Eu(Lys-GlutA-H(2,2)-1,2-HOPO)] was essentially identical. The overall luminescence quantum yields, Φ_{tot}, were determined using quinine sulfate in 0.5 M H_2SO_4 as a reference, and were evaluated to be 4.3% and 4.2% respectively for the [Eu(Lys-H(2,2)-1,2-HOPO)] and the [Eu(Lys-GlutA-H(2,2)-1,2-HOPO)] complexes in 0.1 M TRIS buffered aqueous solution at pH 7.4. These are identical within experimental error, and are slightly higher than the parent form of the complex. The observed increase may be due to a slightly more shielded environment for the Eu(III) cation, because of the additional steric bulk of the alkyl linked pendant amine or carboxylate arms, which would contribute toward reducing the number of nearby aqueous solvent molecules in the second solvation sphere of the complex.

The luminescence lifetimes of the Eu(III) centered emission at 612 nm for each of the new pendant armed octadentate complexes were evaluated in 0.1 M TRIS buffered aqueous solution at pH 7.4, and these results are summarized in Table 2. Notably, the luminescence lifetimes of these two new compounds are almost identical, and remain unchanged when compared to the parent [Eu(H(2,2)-1,2-HOPO)(H$_2$O)] complex. Using the corresponding luminescence lifetimes measured in deuterated solvent allowed us to estimate "q", the number of bound inner sphere solvent molecules, using the improved empirical Horrock's equation.[30] As was the case for the parent [Eu(H(2,2)-1,2-HOPO)(H$_2$O)] complex, this analysis reveals the presence of a single inner sphere water molecule, also contributing toward the lower overall quantum yield values, Φ_{tot}, when compared to 5LIN^{Me}-1,2-HOPO complexes of Eu(III), because of well-known non-radiative quenching by bound inner sphere solvent water molecules. This increase in non-radiative quenching of Eu(III) luminescence is reflected in a higher value for k_{nr}, the non-radiative deactivation rate constant, which was determined together with the radiative decay rate constant, k_r, following the work of Verhoeven et al.[31]

(28) Latva, M. T. H.; Mukkala, V.-M.; Matachescu, C.; Rodriguez-Ubis, J. C.; Kankare, J. *J. Lumin.* **1997**, *75*, 149–169.
(29) de Sa, G. F.; Malta, O. L.; de Mello Donega, C.; Simas, A. M.; Longo, R. L.; Santa-Cruz, P. A.; da Silva, E. F., Jr. *Coord. Chem. Rev.* **2000**, *196*, 165–195.
(30) Supkowski, R. M.; Horrocks, W. D., Jr. *Inorg. Chim. Acta* **2002**, *340*, 44–48.
(31) Werts, M. H. V.; Jukes, R. T. F.; Verhoeven, J. W. *Phys. Chem. Chem. Phys.* **2002**, *4*, 1542.

Table 2. Summary of Experimental and Calculated Photophysical Parameters for Various 1,2-HOPO Based Eu(III) Complexes in 0.1 M TRIS Buffered Aqueous Solution, pH 7.4

complex	λ_{max} (nm)	ε_{max} (M^{-1} cm^{-1})	Φ_{tot} (H_2O) (%)	τ_{obs} H_2O {D_2O} (msec)	q calcd	k_r (ms^{-1}) calcd	k_{nr} (ms^{-1}) calcd	Φ_{Eu} calcd	η_{sens} calcd
[Eu(5LIN^{Me}-1,2-HOPO)$_2$]	332	18,750	17.3	0.73 {1.00}	0.1	0.61	0.77	0.442	0.391
[Eu(H(2,2)-1,2-HOPO)]	341	18,200	3.6	0.48 {1.22}	1.0	0.375	1.75	0.178	0.202
[Eu(Lys-H(2,2)-1,2-HOPO)]	342	18,400	4.3	0.47 {0.99}	0.9	0.335	1.79	0.158	0.272
[Eu(Lys-GlutA-H(2,2)-1,2-HOPO)]	342	18,350	4.2	0.46 {0.98}	0.9	0.343	1.83	0.158	0.266

and Beeby et al.,[32] and a complete summary of these data are also reported in Table 2.

Turning once again to the parent H(2,2)-1,2-HOPO ligand, we have prepared the Gd(III) complex to investigate the energetic position of the lowest energy ligand-centered triplet state. This metal cation has a similar size and atomic weight when compared to Eu(III), but lacks an appropriately positioned electronic acceptor level, making it amenable to the observation of phosphorescence from the ligand's lowest energy T_1 state at low temperature. Measurements were performed at 77 K in a solid matrix of 1:1 (v/v) MeOH:EtOH which also contained about 5% (v/v) of 1.0 M TRIS buffered aqueous solution at pH 7.4 to enable pH control of the otherwise nonaqueous solvent. The resulting spectrum for [Gd(H(2,2)-1,2-HOPO)(H_2O)] (Supporting Information, Figure S2) shows an intense unstructured emission band apparent from 450 to 650 nm, which we attribute to phosphorescence from the ligand. The lowest energy zero phonon ($v_{0-0'}$) band of the T_1 state was estimated by spectral deconvolution of the 77 K luminescence signal into several overlapping Gaussian functions, and the lowest energy peak was evaluated to be about 20,385 cm^{-1}. Importantly, the position of this state is about 875 cm^{-1} lower in energy, when compared to the values obtained via identical analysis[25] of a bis(tetradentate) Gd(III) complex which lacks an alkyl amine in the ligand backbone. In the latter cases, the energy gap between the lowest energy T_1 triplet state and the $^5D_1$ accepting state is optimal at about 2230 cm^{-1}. The decrease of this energy gap can be expected to significantly decrease the sensitization efficiency for the H(2,2)-1,2-HOPO complex (and pendant armed derivatives), which is corroborated by lower values of η_{sens} as shown in Table 2, and is also in accordance with our TD-DFT calculations, strongly suggesting that protonation of the adjacent amines influences the energetic position of the triplet state, and hence the overall luminescence performance of Eu(III) in 1,2-HOPO complexes containing alkyl amine backbones.

Bioconjugation Studies. Lastly, in a proof of principle experiment, a bioconjugate of the carboxy functionalized [Eu(Lys-GlutA-H(2,2)-1,2-HOPO)(H_2O)] complex was prepared with Streptavidin (SAv), a 52.8 kDa tetrameric protein commonly utilized in molecular biology because of its extraordinarily strong non-covalent interaction with biotin. This SAv-[Eu(Lys-GlutA-H(2,2)-1,2-HOPO)-(H_2O)$_q$] bioconjugate was prepared using standard NHS activated coupling techniques, and was purified from unreacted starting materials using gel filtration. The degree of labeling (DOL) of the purified bioconjugate

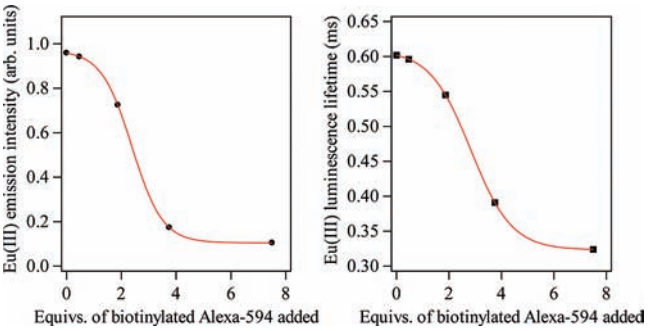

Figure 7. LRET assay plots from a 500 nM solution of SAv-[Eu(Lys-GlutA-H(2,2)-1,2-HOPO)] in 0.1 M TRIS buffered aqueous solution at pH 7.4 (**a**) Eu(III) centered emission intensity and (**b**) Eu(III) luminescence lifetime (λ_{ex} = 335 nm) upon incremental addition of 0, 0.5, 2.0, 3.75, and 7.5 mol equiv of a biotinylated Alexa Fluor 594 organic dye.

was determined to be about 2.3 from analysis of the UV−visible absorption spectrum at 280 and 342 nm, corresponding to the λ_{max} of the protein and complex, respectively. The steady state Eu(III) centered emission spectrum of the SAv-[Eu(Lys-GlutA-H(2,2)-1,2-HOPO)-(H_2O)$_x$] bioconjugate upon excitation of the 1,2-HOPO chromophore at about 340 nm was unchanged when compared to that of the [Eu(Lys-GlutA-H(2,2)-1,2-HOPO)(H_2O)$_x$] complex. The luminescence lifetime of the Eu(III) bioconjugate was also determined at λ_{em} = 612 nm, and yielded a satisfactory fit to a monoexponential decay, with an observed lifetime of τ_{obs} = 0.60 ms. In comparison to the unlabeled complex (τ_{obs} = 0.46 ms), we attribute the slight increase in lifetime as a result of the more shielded protein environment, which serves to protect the complex from deactivation by non-radiative interactions with the solvent.

Using a commercially available biotinylated Alexa Fluor 594 fluorescent dye, we have examined the photophysical changes evident upon interaction of these molecules in buffered aqueous solution at pH = 7.4 using both steady state and time-resolved luminescence. This organic chromophore was chosen as an acceptor specifically because of its good Förster overlap with the Eu(III) centered emission of the complex. The resulting plot of observed overall luminescence upon the addition of increasing equivalents of the biotinylated Alexa Fluor 594 dye (Supporting Information, Figure S3), and the intensity of the Eu(III) emission, obtained by subtracting the known emission of the organic dye, versus added equivalents is shown in Figure 7. A sigmoidal decrease in Eu(III) centered emission was observed which clearly plateaus after about 4 equiv of Alexa Fluor 594, consistent with the tetrameric nature of the SAv-biotin interaction. Furthermore, by monitoring the luminescence lifetimes, we observed an almost identical decrease in lifetime from about 0.6 to 0.3 ms upon addition of up to about 4 equiv of

(32) Beeby, A.; Bushby, L. M.; Maffeo, D.; Williams, J. A. G. *J. Chem. Soc., Dalton Trans.* **2002**, 48.

biotinylated Alexa Fluor 594, consistent with quenching of the Eu(III) centered luminescence by intramolecular energy transfer. The long-lived Eu(III) signal was completely quenched upon further addition of the biotinylated Alexa Fluor 594 organic dye. The intramolecular nature of the LRET quenching was verified by a titration in the presence of an initially added excess of unlabeled biotin. In this case, no significant changes were observed in the lifetime of the Eu(III) signal because of presaturation of the available Streptavidin binding sites.

Conclusions

The 1-hydroxypyridin-2-one chelate group has proven to be a remarkably efficient sensitizer for long-lived Eu(III) luminescence. By using an exclusively oxygen containing donor set, the resulting compounds also form extremely stable complexes in aqueous solution with oxophilic lanthanides, essential for their practical usage in bioassay applications, where complexes must be highly resistant toward decomplexation, even in the presence of strong competitors such as EDTA commonly used in biotechnology. Despite the presence of a single inner sphere water molecule, these compounds exhibit useful quantum yields in aqueous solution of $\Phi_{tot} \sim 4\%$. Furthermore, we have now developed synthetic methodologies toward the preparation of pendant armed versions of these ligands, containing either terminal amine or carboxylate functional groups, suitable for the attachment to relevant biomolecules, and have demonstrated the use of the resulting bioconjugate in a simple LRET bioassay platform.

Through a thorough understanding of their solution behavior, we have also identified that the use of basic alkyl amine backbones to link adjacent 1,2-HOPO chelates can influence the resulting triplet energies of the chromophore, resulting in less efficient sensitization of the bound Eu(III) metal center. As a result, we are now exploring methodologies to exclude the remaining inner sphere water molecule (by introducing additional steric bulk at the "open" face of the tetrapodal complexes), and to replace the alkyl amine backbone groups with either branched carbon linkages or by utilizing less basic amide groups,[33] with the hope of preparing new octadentate 1,2-HOPO derivatives, whose complexes with Eu(III) have overall quantum yields more similar to $\Phi_{tot} \sim 20\%$ obtained for related bis(tetradentate) complex topologies.

Acknowledgment. This work was partially supported by the NIH (Grant HL69832) and supported by the Director, Office of Science, Office of Basic Energy Sciences, and the Division of Chemical Sciences, Geosciences, and Biosciences of the U.S. Department of Energy at LBNL under Contract No. DE-AC02-05CH11231. This technology is licensed to Lumiphore, Inc. in which some of the authors have a financial interest. Financial support was provided to C.J.J. by the German Research Foundation (DFG).

Supporting Information Available: MM2 optimized molecular models of protonated complexes, low temperature luminescence spectra of Gd(III) complex, and emission spectra from LRET assay. This material is available free of charge via the Internet at http://pubs.acs.org.

(33) Moore, E. G.; D'Aleo, A.; Xu, J.; Raymond, K. N. *Aust. J. Chem.* **2009**, *62*, 1300–1307.